

## Counterion condensation in ionic micelles as studied by a combined use of SANS and SAXS

V K ASWAL<sup>1</sup>, P S GOYAL<sup>2</sup>, H AMENITSCH<sup>3</sup> and S BERNSTORFF<sup>4</sup>

<sup>1</sup>Solid State Physics Division; <sup>2</sup>IUC-DAEF, Mumbai Centre, Bhabha Atomic Research Centre, Mumbai 400 085, India

<sup>3</sup>Institute of Biophysics and X-ray Structure Research, Austrian Academy of Sciences, Graz, Austria

<sup>4</sup>Sincrotrone Trieste, Trieste, Italy

**Abstract.** We report a combined use of small-angle neutron scattering (SANS) and small-angle X-ray scattering (SAXS) to the study of counterion condensation in ionic micelles. Small-angle neutron and X-ray scattering measurements have been carried out on two surfactants cetyltrimethylammonium bromide (CTABr) and cetyltrimethylammonium chloride (CTACl), which are similar but having different counterions. SANS measurements show that CTABr surfactant forms much larger micelles than CTACl. This is explained in terms of higher condensation of  $\text{Br}^-$  counterions than  $\text{Cl}^-$  counterions. SAXS data on these systems suggest that the  $\text{Br}^-$  counterions are condensed around the micelles over smaller thickness than those of  $\text{Cl}^-$  counterions.

**Keywords.** Small-angle neutron scattering; small-angle X-ray scattering; charged micelle; counterion condensation.

**PACS Nos** 61.12.Ex; 82.70.Uv; 82.70.Dd

### 1. Introduction

The very popular notion of effective polyion charge is a concept of fundamental importance in the field of highly charged colloidal or polyelectrolyte solutions. In such suspensions, the electrostatic coupling between oppositely charged species induces a strong accumulation of counterions, referred to as counterion condensation, in the vicinity of the macroion surface. The basic idea is thus to consider the structural colloid and the condensed counterionic shell as a whole which carries an effective charge ( $Z_{\text{eff}}$ ) much weaker than the structural one ( $Z_{\text{str}}$ ). Consequently, as far as the colloid is concerned, all Debye–Hückel-like linearized approaches which fail to correctly treat the nonlinear condensation phenomenon, can still be used if  $Z_{\text{str}}$  is more or less replaced by  $Z_{\text{eff}}$ . The counterions are condensed around the charged particles according to their electrostatic energy. The counterion distribution is given by the Poisson–Boltzmann equation [1]. This equation has no analytical solutions and different types of approximations are used in order to solve it analytically or

numerically. These results could be verified by the experimental measurements of counterion condensation. We have made combined use of the small-angle neutron scattering (SANS) and small-angle X-ray scattering (SAXS) to the study of the counterion condensation in ionic micelles. While SANS determines the shape and size of the micelles, SAXS in combination with SANS is used to get information on counterion condensation (especially when the atomic number of counterions is high).

Surfactant molecules such as cetyltrimethylammonium bromide (CTABr) ionize in aqueous solution and the corresponding micelles are aggregates of  $\text{CTA}^+$  ions. The micelle is charged and is called an ionic micelle [2]. The  $\text{Br}^-$  ions, known as counterions, tend to stay near the  $\text{CTA}^+$  micellar surface. The counterions located at short enough distances from the colloidal surface feel a very strong electrostatic attraction compared with the thermal energy  $k_B T$  and these counterions are called as bound to or condensed on the colloid. In ionic micellar solutions, the counterion condensation plays a very important role in deciding the effective charge on the micelle and hence the formation, structure and interaction of the micelles [3–6]. In the present work, we show a combined use of SANS and SAXS to explain the role of counterion condensation to decide the micellar structure.

## 2. Experiment

Small-angle neutron scattering experiments were carried out using SANS diffractometer at the Swiss Spallation Neutron Source SINQ, Paul Scherrer Institute. The wavelength of the neutron beam was 4.8 Å and the experiments were performed at two different samples to detector distances of 2 and 8 m to cover a  $Q$  range of 0.007 to 0.30 Å<sup>-1</sup>. Small-angle X-ray scattering experiments were performed at the SAXS beamline of synchrotron source ELETTRA, Trieste, Italy. The wavelength of X-ray beam was 1.54 Å and the data were recorded in the  $Q$  range of 0.015 to 0.3 Å<sup>-1</sup>. The surfactants used were obtained from Aldrich. The samples were prepared by dissolving known amount of surfactants in D<sub>2</sub>O. The use of D<sub>2</sub>O as solvent instead of H<sub>2</sub>O provides better contrast in neutron experiments. In SAXS experiments, the choice of solvent D<sub>2</sub>O or H<sub>2</sub>O does not matter.

## 3. Small-angle scattering

SANS and SAXS have been referred to as small-angle scattering. The experimental details and the data analysis methods used in the two techniques are similar and the only difference is in the radiation used. As it will be discussed below, because of differences in their interactions with matter the contrast factors and the scattering length densities will be different for neutrons and X-rays.

The small-angle scattering intensity  $I(Q)$  as a function of scattering vector  $Q(=4\pi \sin \theta/\lambda)$ , where  $2\theta$  is the scattering angle and  $\lambda$  is the wavelength of incident radiation) for a micellar solution can be expressed as [7]

$$I(Q) = nP(Q)S(Q), \quad (1)$$

where  $n$  is the number density of the particles.  $P(Q)$  is the intraparticle structure factor and depends on the shape and size of the particles.  $S(Q)$  is the interparticle structure factor and is decided by the spatial distribution of the particles.  $P(Q)$  is given by the integral

$$P(Q) = \left| \int (\rho(r) - \rho_s) \exp(i\mathbf{Q} \cdot \mathbf{r}) d\mathbf{r} \right|^2. \quad (2)$$

In the simplest case of a monodispersed system of homogeneous spherical particles with a radius  $R$ ,  $P(Q)$  is given by

$$P(Q) = (\rho - \rho_s)^2 V^2 \left[ \frac{3J_1(QR)}{QR} \right]^2, \quad (3)$$

where  $V = (4/3)\pi R^3$ ,  $\rho_s$  is the scattering length density of the solvent and  $\rho$  is the mean scattering length density of the particle.

The expression for  $S(Q)$  depends on the relative positions of the particles. In case of isotropic system,  $S(Q)$  can be written as

$$S(Q) = 1 + 4\pi n \int (g(r) - 1) \frac{\sin Qr}{Qr} r^2 dr, \quad (4)$$

where  $g(r)$  is the radial distribution function.  $g(r)$  is the probability of finding another particle at a distance  $r$  from a reference particle centered at the origin. The details of  $g(r)$  depend on the interaction potential  $U(r)$  between the particles. For the results reported in this paper,  $U(r)$  was assumed to be screened Coulomb potential and  $S(Q)$  was calculated under mean spherical approximation [4–6].

The term  $(\rho - \rho_s)^2$  is referred as a contrast factor. The above equations are valid both for the SAXS and the SANS experiments. The contrast factor, however, depends on the radiation used. The values of  $\rho$  and  $\rho_s$  depend on the chemical composition of the micelle and the solvent and are different for neutrons and X-rays. The differences in  $\rho$  values for neutrons and X-rays arise from the fact that while neutrons are scattered by the nucleus of an atom, the X-rays are scattered by the electron clouds around the nucleus. It is seen that as one goes across the periodic table, the neutron scattering lengths vary in a random way and the X-ray scattering lengths increase with the atomic number of the atom. For example, unlike X-rays where  $\rho_s(\text{H}_2\text{O}) = \rho_s(\text{D}_2\text{O})$ , the values of  $\rho_s$  changes significantly for neutrons when solvent is changed from  $\text{H}_2\text{O}$  to  $\text{D}_2\text{O}$ . X-rays are scattered more strongly from heavy elements (e.g.  $\text{Cl}^-$ ,  $\text{Br}^-$  etc.) as compared to light elements such as C, H etc. That is while X-rays are scattered by the counterions and neutrons by the core of the micelle [8,9].

#### 4. Results and discussion

Figure 1 shows the comparison of SANS and SAXS data on 100 mM CTABr micellar solution. The insets show the variation of scattering length densities for different components of the micelles corresponding to the radiation used. The contrast for

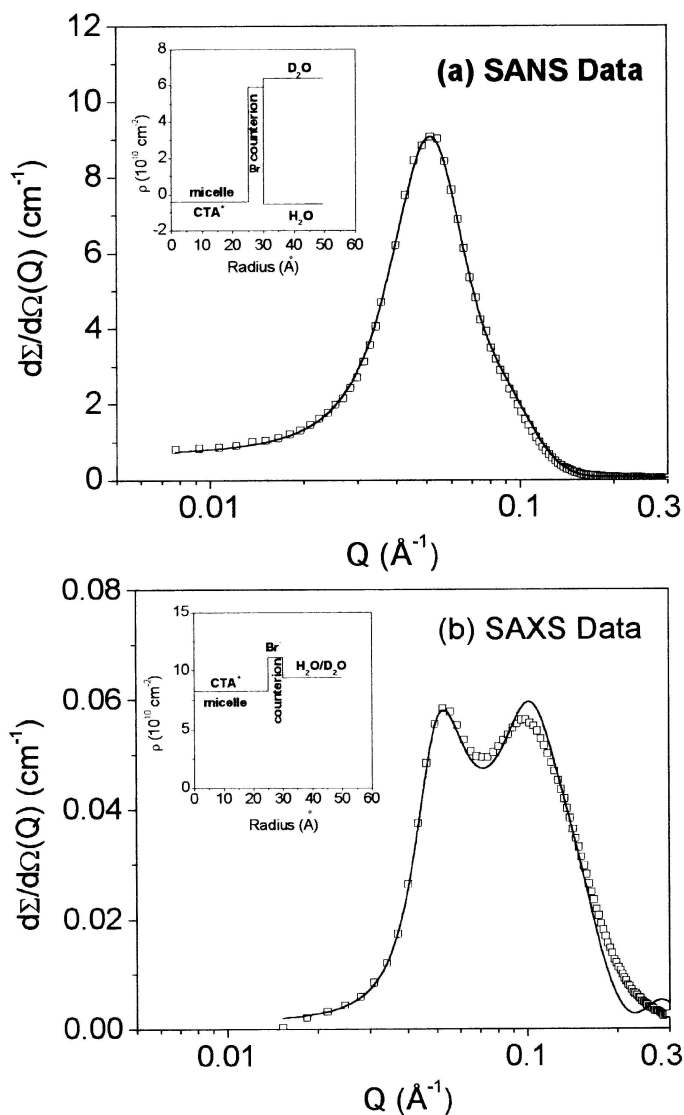


**Figure 1.** Comparison of (a) SANS and (b) SAXS data from 100 mM CTABr. The insets show the variation of scattering length densities for different components of the micelles corresponding to the radiation used.

any component depends on the square of the difference of scattering length densities of that component and solvent. It is clear from the variation of scattering length density for neutrons that there exists a very strong contrast for the micelles in D<sub>2</sub>O with respect to that for the counterions. This makes the scattering from counterions negligible and neutrons only see the core of the micelles. However, the same is not the case with X-rays. There exists a similar contrast for counterions

as well as for the core of the micelles. It is seen that both the SANS and SAXS data show a correlation peak at  $Q \sim 0.05 \text{ \AA}^{-1}$ , which is due to peak from the interparticle structure factor  $S(Q)$  [3–6]. The fact that the average distance between the micelles mainly decides the position of the correlation peak, it is independent of the radiation used. The peak usually occurs at  $Q_m \sim 2\pi/d$ , where  $d$  is the average distance between the micelles and  $Q_m$  is the value of  $Q$  at the peak position. The second peak in the SAXS data arises from scattering of shell-like structure of the condensed counterions around the micelles [8,9].

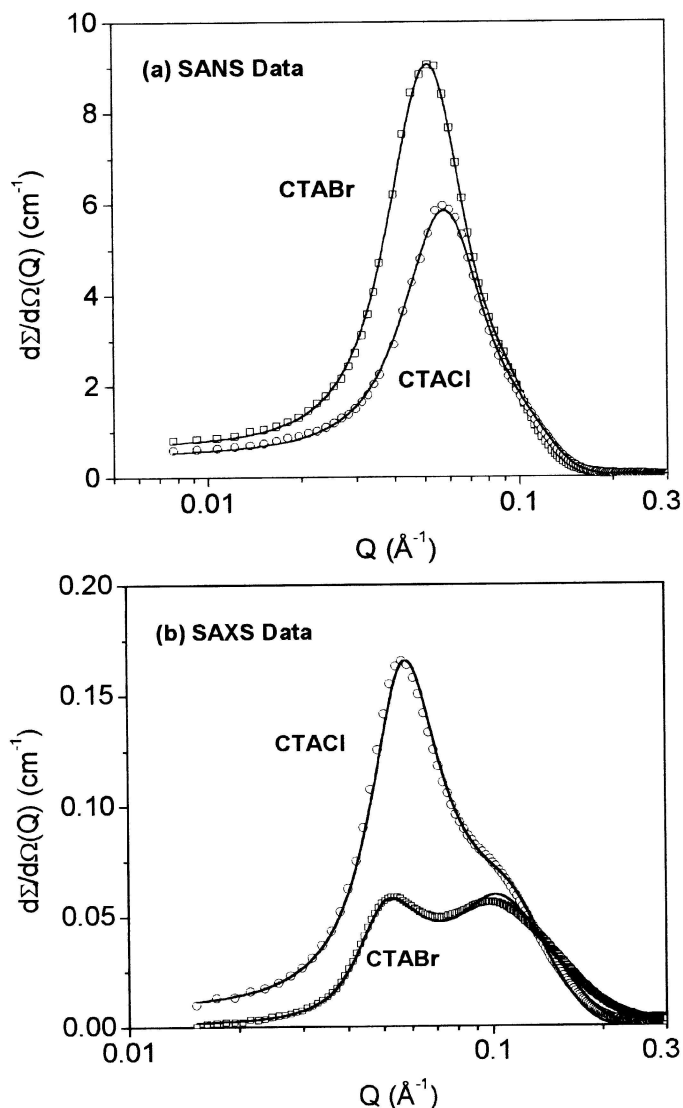


**Figure 2.** Comparison of (a) SANS and (b) SAXS data for 100 mM CTABr and CTACl micellar solutions.

The analysis of SANS data using eq. (1) determines the shape and size of the micelles [3–6]. It is found that the micelles are prolate ellipsoidal with the semimajor axis ( $a$ ) = 40.2 Å and semiminor axis ( $b = c$ ) = 24.0 Å, respectively. The counterion condensation per surfactant molecule on the micelles has a value of about 77%. The above structure and interaction information about the micelles as obtained from SANS is used to fit the SAXS data and the thickness of the condensed counterions around the micelles is obtained as an additional parameter. The calculated value of the thickness over which the Br<sup>−</sup> counterions are condensed is 4.2 Å. The fact that ionic radius of bare Br<sup>−</sup> ion is 1.95 Å, this suggests that most of condensed Br<sup>−</sup> ions reside in about a single-layer of counterions around the micelle.

Figure 2 shows the comparison of SANS and SAXS data for CTABr and CTACl micellar solutions. SANS suggests the formation of much smaller micelles for CTACl ( $a = 29.1$  Å,  $b = c = 23$  Å) than CTABr [6]. This is explained due to the lower condensation of Cl<sup>−</sup> counterions (72%) on the micelles. On the other hand, SAXS data suggest that counterions be condensed over larger thickness for CTACl micelles. It is found that the thickness of condensed Cl<sup>−</sup> counterions around CTACl micelle is 4.6 Å, which is about 30% larger than the single-layer thickness of condensed Cl<sup>−</sup> counterions. This result along with the one reported in the earlier section suggests that Cl<sup>−</sup> counterions are less densely condensed compared to Br<sup>−</sup> counterions around the micelles. To our knowledge, this is the first experimental observation of the above fact.

## 5. Conclusion

A combined use of SANS and SAXS has been made to study the counterion condensation in ionic micelles. While neutron scattering in micellar solutions is from the core of the micelle, X-rays are largely scattered by counterions, especially when the counterion has a large atomic number (e.g. Br<sup>−</sup>). It is found that the difference in the condensation of Br<sup>−</sup> and Cl<sup>−</sup> counterions around the micelles gives rise to the different structure of CTABr and CTACl micelles.

## References

- [1] L Belloni, *Coll. Surf.* **A140**, 227 (1998)
- [2] Y Chevalier and T Zemb, *Rep. Prog. Phys.* **53**, 279 (1990)
- [3] V K Aswal, P S Goyal and P Thiyagarajan, *J. Phys. Chem.* **102**, 2469 (1998)
- [4] V K Aswal and P S Goyal, *Phys. Rev.* **E61**, 2947 (2000)
- [5] V K Aswal and P S Goyal, *Chem. Phys. Lett.* **364**, 44 (2002)
- [6] V K Aswal and P S Goyal, *Phys. Rev.* **E67**, 051401 (2003)
- [7] S H Chen and T L Lin, in *Methods of experimental physics* edited by D L Price and K Skold (Academic Press, New York, 1987) vol. 23B, p. 489
- [8] C F Wu, S H Chen, L B Shih and J S Lin, *Phys. Rev. Lett.* **61**, 645 (1988)
- [9] V K Aswal, P S Goyal, S De, S Bhattacharya, H Amenitsch and S Bernstorff, *Chem. Phys. Lett.* **329**, 336 (2000)